Continuous-wave laser spectrometer automatically aligned and continuously tuned from 11.8 to 16.1 μm by use of diode-laser-pumped difference-frequency generation in GaSe

Roger S. Putnam and David G. Lancaster

We report a fully automated mid-IR difference-frequency spectrometer with a spectral resolution under 70 MHz pumped by a pair of conventional room-temperature 800–900-nm diode lasers. 0.1 μW of tunable cw radiation is produced from incident-diode powers of 120 and 75 mW. The system has computer-controlled beam alignment with compact CCD cameras, motorized mirrors and positioners to obtain 0.01° crystal-angle positioning, 4-μm beam overlap at the nonlinear crystal, and automated diode laser beam collimation. Computer-operated frequency control uses temperature tuning and current tuning of the free-running diode lasers. The system has been demonstrated by successfully scanning, without any human intervention, 64 randomly selected acetylene absorption lines between 12 and 15 μm. Spectral scans of ammonia are also presented. This mid-IR spectrometer is suitable for fully automated spectroscopy of an unlimited list of mid-IR frequencies and has the potential to detect any trace gas that has an acceptable absorption line within the large tuning range.

OCIS codes: 010.1120, 120.6200, 190.2640, 300.6360, 140.2020, 300.6340.

1. Introduction

Agile and precise measurement of trace air-pollutant concentrations and fluxes is a critical requirement for both the elucidation and the remediation of environmental problems. This is true for problems ranging from global-scale issues such as stratospheric ozone depletion and greenhouse gas buildup to local pollution issues such as urban smog and toxic contamination. Examples include SO_2, NH_3, H_2O_2, HNO_3, HNO_2, N_2O, CH_4, O_3, CO_2, NO, NO_2, HCN, C_2H_2, C_2H_6, CCl_4, H_2CO, HNO_4, ClO, OCS, PH_3, HOCl, and chlorofluorocarbons. Trace-gaseous-species detection and quantification are also important for the characterization and the control of combustion-driven energy and propulsion sources and key industrial processes, including plasma and chemical vapor reactors for semiconductor device production.

Tunable IR laser differential absorption spectroscopy has proved to be a powerful technique for accurately determining the real-time concentrations and fluxes of trace pollutants in both point-monitoring and open-path configurations.[1,2] Some of these systems utilize tunable III–V diode lasers in the 0.7–2.0-μm near-IR region, but the most sensitive systems use cryogenically cooled lead-salt diode lasers in the 3–20-μm mid-IR region since molecular absorption line strengths are typically 20–200 times greater in this wavelength region where most pollutant molecules have their fundamental vibrational and rotational bands. However, these mid-IR lead-salt diode lasers have a number of operational drawbacks that restrict the utility of current instruments. These include the need for cryogenic cooling, narrow tuning ranges between mode hops, variable and degraded tuning characteristics that are due to material diffusion, and narrow single-diode frequency coverage which limits the system's flexibility in measuring multiple trace species. Moreover, present lead-salt laser-based systems lack automated optical alignment and frequency tuning, which then often require the attention of technically sophisticated personnel.

When this research was performed, the authors were with Aerodyne Research, Incorporated, 45 Manning Road, Billerica, Massachusetts 01821-3976. D. G. Lancaster is now with Rice Quantum Institute, Rice University, 6100 Main Street, Houston, Texas 77005.

Received 31 March 1998; revised manuscript received 12 June 1998.

0003-6935/99/091513-10$15.00/0

Recently, quantum-cascade mid-IR lasers have debuted[3] in the laboratory at progressively higher temperatures[4] with the expectation that room-temperature operation will become practical. These have been demonstrated under laboratory conditions at −17 to +6 °C with a 1% duty cycle to scan CH_4 and N_2O spectrally and to measure N_2O accurately near 8 μm despite a 720-MHz linewidth that is due to pulsed operation.[5] Also, cw operation of optical parametric oscillators has been demonstrated in periodically poled $LiNbO_3$,[6] which is limited by absorption to produce wavelengths below 4.8 μm. Another mid-IR competitor is the Fourier-transform infrared spectrometer with resolutions generally greater than 1 cm^{-1}, which is roughly 20 times the Doppler- and the pressure-broadened linewidth that we use for optimized laser trace-gas detection with a single absorption line.

Difference-frequency generation (DFG) was first demonstrated for molecular spectroscopy by Pine,[7] who used an Ar^+ laser and a tunable dye laser in a $LiNbO_3$ crystal. The system was tunable from 2.2 to 4.2 μm, had a resolution of 15 MHz, and was demonstrated by scanning the absorption lines of H_2O, NH_3, CH_4, and N_2O. That system had the advantages of being cw and smoothly and continuously tunable; but the size, weight, and power consumption of the drive lasers posed significant disadvantages for portable spectrometer applications. It is relatively simple to obtain high power by means of DFG with pulsed-drive lasers, but the resulting broad spectra are inadequate for measuring 30-MHz-wide absorption features and for separating small trace-gas absorption lines from the wide absorbing wings of predominant species.

The availability of high-power, narrow-bandwidth, room-temperature diode lasers[8] now makes possible a compact and widely tunable mid-IR spectrometer by DFG with two diode lasers,[9–12] and the emergence of high-power diode lasers in the 600–1500-nm region combined with nonlinear materials such as $ZnGeP_2$, $AgGaSe_2$, $AgGaS_2$, GaSe, and periodically poled $LiNbO_3$ provides access to the entire 2–18-μm spectral range. Our choice of GaSe[13] for the mid-IR spectrometer results from the combined requirements of a large nonlinearity (54 pm/V),[14] a real transparency at 800–900 nm for the drive beams and at 7–16 μm for the mid-IR output, and a birefringence that permits angle tuning any pair of 800–900-nm drive wavelengths into a 7–16-μm idler wavelength. The flaw in this choice appears to be the GaSe crystal quality, which can limit the effective length of the nonlinear interaction to several millimeters, although an improvement in crystal-lattice quality by doping has been reported.[15] Our requirement that crystal-angle tuning be used to (critically) phase match any realistic pair of drive frequencies from the two diode lasers results in a shorter interaction length and a lower conversion efficiency than is available with 90° noncritical phase matching.[16,17] However, our choice of angle tuning permits generating the particular desired mid-IR frequency by any pair of diode laser frequencies that are available and happen to have the correct frequency difference: This is a great advantage when we are dealing with simple diode lasers that do not have smooth temperature tuning but show mode hops; Fig. 1 shows that there are typically hundreds of frequency pairs available from the two diode lasers to produce any particular IR frequency when a diode temperature-tuning range of 0–40 °C is used.

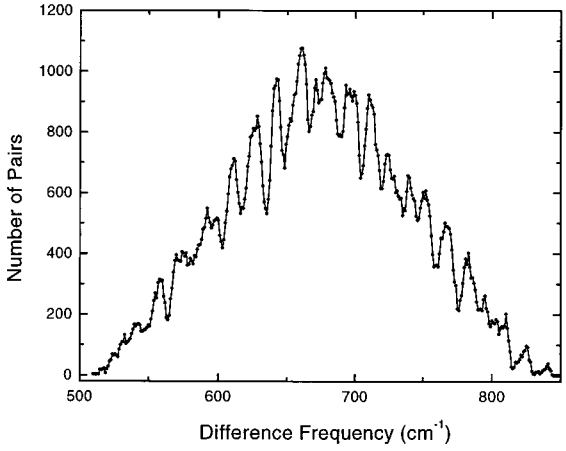

Fig. 1. Experimentally measured tuning data for the two diode lasers at the 130-mW power level was recorded from 0 to 40 °C. All possible combinations of the available frequencies were checked, and the number of different pairs found that will produce a given mid-IR frequency is shown in the figure. Hundreds of frequency pairs produced by the two diode lasers are available to produce any desired mid-IR frequency.

2. System Concept

The system was conceived as a prototypical universal trace-gas monitor and laser spectrometer for the mid-IR region between 7 and 16 μm and is intended to require no human intervention while scanning an unlimited list of spectral regions, to record the spectra, and, in the case of trace-gas detection, to find and to extract the fractional absorption of the chosen line.

The mid-IR frequency is generated by DFG in an angle-tuned GaSe crystal driven by a pair of diode lasers at 809 and 856 nm. The temperature-tuning characteristics of these free-running diode lasers are automatically recorded by the system, and the resulting look-up tables are used in selecting the best pair of diode laser frequencies to produce any desired mid-IR frequency. Compelling the diode lasers to produce the chosen frequencies is a complex process and is made possible by the fact that more than 100 similar pairs will give the same desired mid-IR frequency and that the use of angle tuning (instead of 90° phase matching) permits any such pair to be utilized (see Fig. 1).

The past need for technically sophisticated personnel to tune the laser frequency over the gas absorption line as well as to realign the optical system occasionally has driven the requirement for fully automated tuning and alignment, including the task of identifying the correct absorption line. Our present

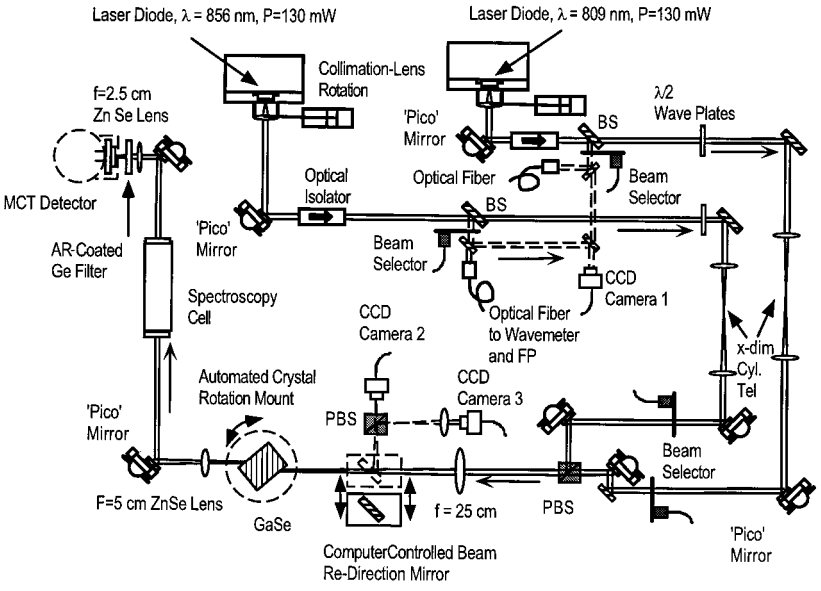

Fig. 2. Optical setup includes two temperature-controlled diode lasers with automated collimation at 809 and 856 nm, eight motorized picomirrors, single-mode fiber coupling, optical isolators, horizontal cylindrical-lens telescopes, three CCD cameras, a polarizing beam splitter (PBS) for combining the drive beams, a motorized rotary mount with a 5-mm GaSe crystal, a deflection mirror on a swing arm, a 25-cm focusing lens, a 5-cm ZnSe mid-IR collimating lens, a 2.5-cm detector focusing lens, an AR-coated Ge filter, and a 10–16-μm HgCdTe (MCT) detector. FP, Fabry–Perot spectrum analyzer.

system sets the mid-IR frequency with an absolute accuracy of ~50 MHz, uses pattern recognition on the spectral scan to locate the center of the absorption line, and uses a nonlinear fitting routine to extract the actual fractional absorption.

The correct overlap and angular alignment of the drive beams in the GaSe crystal, as well as an accurately predicted and subsequently optimized crystal angle, are required for DFG. These requirements are compounded by the wide tuning range that both changes the IR exit angle at the crystal and results in physical movement of the lasers diodes over the large 0–40 °C tuning range. The optical system is automatically aligned by four CCD cameras controlling eight motorized mirror mounts, by calculation of the frequency-dependent crystal angle and the temperature-dependent diode laser collimating-lens position, and by optimization routines that maximize the IR output power.

3. Experimental Setup

A. Difference-Frequency Generation Layout

A schematic of the DFG system is shown in Fig. 2, including pump (extraordinary-beam) and signal (ordinary-beam) diode lasers that are nominal 150-mW narrow-bandwidth diodes at 856 and 809 nm (SDL 5400 series). Two Newport 700C thermoelectrically controlled mounts are driven by an IEEE general-purpose-interface-bus (GPIB) interfaced modular dual-diode controller (ILX Lightwave LDC-3900). The diode outputs are collimated by Geltech aspheric lenses (f = 2.75 mm, N.A. = 0.65) that are held in a threaded rotating mount that allows fine adjustment of the diode–lens spacing by computer-controlled linear translation stages (National Aperture): This was necessary to compensate for the variation in the diode position as a function of the thermoelectrically cooled mount temperature. The diode laser beams are reflected off computer-controlled mirrors (New Focus) and pass through optical isolators and λ/2 wave plates to the correct polarizations for type I phase matching in the GaSe crystal (Eksma[18]). A portion of the mixing beams are reflected by an antireflection- (AR) coated glass wedge to a CCD camera and to a gradient-index lens that couples into an optical fiber. The CCD image is used for monitoring the beam collimation and alignment. The fiber-coupled light reaches a wavemeter for diode frequency monitoring (Burleigh 1500; 0.001-cm^{-1} accuracy) and a scanning Fabry–Perot spectrum analyzer with variable mirror spacing for monitoring the diodes' spectral characteristics, especially the relaxation sidebands spaced at 1–3 GHz. Motorized shutters allow either beam to be selected. Each diode laser beam is passed through a cylindrical telescope to reduce the horizontal dimension and to correct astigmatism, and a vertical Gaussian field radius of 1.2 to 1.6 mm is used at the 25-cm focusing lens, which produces a focused spot size of ~50 μm (vertical field radius). The calculated optimum is ~44 μm in the 5-mm crystal. The two orthogonally polarized diode beams are combined in a polarizing beam splitter.

The angle-phase-matched GaSe crystal is mounted on a compact motorized rotation stage (National Aperture) with an absolute accuracy of 0.01°. The generated mid-IR idler beam is collimated by an f = 5 cm ZnSe lens and is separated from the drive beams by an AR-coated Ge filter. The mid-IR beam passes through the 10-cm absorption cell and is focused by an f-2.5-cm ZnSe lens onto the liquid-N_2-cooled HgCdTe detector (Kolmar) that is optimized for 10–15 μm. One diode laser drive beam is mechanically chopped, and a lock-in amplifier is used with the detector.

The internal phase-matching angle for type I DFG in GaSe is 14.8° at an idler wavelength of 13.9 μm. This results in a 45.7° external angle because the

pure GaSe crystal is soft and cannot be cut at an angle but cleaves in a micalike fashion perpendicularly to the c axis, which then also produces, with a large optical index of 2.8, astigmatic elliptical beams. The external angular-phase-matching sensitivity for our 5-mm GaSe, which has an ordinary-ray idler, was measured as 0.4° FWHM.

B. Electronics

The 166-MHz Pentium control computer includes a Viewpoint Software Solutions framegrabber and software for the various compact CCD alignment cameras, a nuLogic motor controller board to adjust the two collimating lenses and the crystal angle through a National Aperture servoamplifier, an IEEE GPIB interface board, and an input–output (I/O) board for analog output to scan the diode lasers' currents, for analog input from temperature sensors and the amplified Fabry–Perot optical detector, and for digital output to the various small motors and voice coil actuators that operate beam blocks and mirror beam deflectors. A New Focus controller operates the eight motorized mirrors from the GPIB, which also controls the Burleigh 1500 Wavemeter with 0.001-cm^{-1} resolution and the ILX Lightwave LDC-3900 dual-diode-laser current and temperature controller. The focused beams' approaches to the GaSe crystal are observed on a pair of black-and-white monitors, and the mid-IR detector signal is amplified by an ordinary lock-in amplifier.

4. Experimental Results

A. Diode Tuning

The frequency of the laser diodes is principally controlled by changes in the diode temperature and current. The single-longitudinal-mode lasers are characterized by somewhat unpredictable mode hopping and significant hysteresis behavior as a function of temperature, as shown in Fig. 3 of a typical 100-mW device (SDL-5410). Figure 3 also reveals consistently smooth temperature tuning on a particular longitudinal mode. An alternative to simple temperature tuning is to turn the diode current off momentarily, which allows the laser to restart on one of the several available longitudinal modes. This both removes any temperature-tuning hysteresis and typically provides random access to more modes if the current is repeatedly interrupted, as shown in Fig. 4. This technique is most effective if the current interruption is kept below 10 ms, which reduces active thermal-tuning effects at the diode junction.

The pseudo-AR coating (~1%) on the emitting facet of the 150-mW SDL-5400 lasers increases the lasers' sensitivity to externally reflected fields, resulting in mode hops, frequency pulling, and noisy behavior as indicated by the sidelobes at the 1–3-GHz relaxation oscillation frequencies. These are revealed by a scanning Fabry–Perot spectrum analyzer and by subtle, but detectable, amplitude fluctuations. We observed frequency pulling at reflected fractional power levels of $\sim 10^{-8}$. The closely spaced laser collimating lens provides significant optical feedback, which greatly determines which laser modes are available and which are noisy. This fact is exploited to provide better control over the tuning and is discussed in detail in Section 5. Removing the optical feedback from the diode laser window by removing the window changes the erratic temperature-tuning curve in Fig. 5 into a smooth and straight tuning curve.

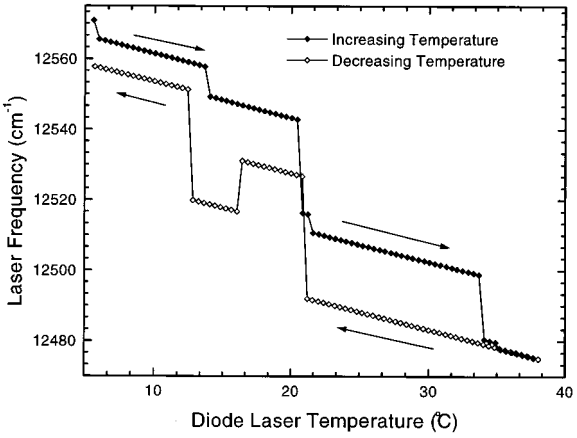

Fig. 3. Temperature tuning of a 100-mW diode laser with a pseudo-AR coating on the emitting facet shows hysteresis and randomly appearing mode hops. The hysteresis was removed when the current was momentarily lowered below threshold, which permits the laser to restart: This also permitted reaching several different modes without changing the temperature. The stability of these mode choices was strongly influenced by optical feedback and was controlled by the position of the collimating lens after the laser window was removed.

The two diode lasers are characterized by a com-

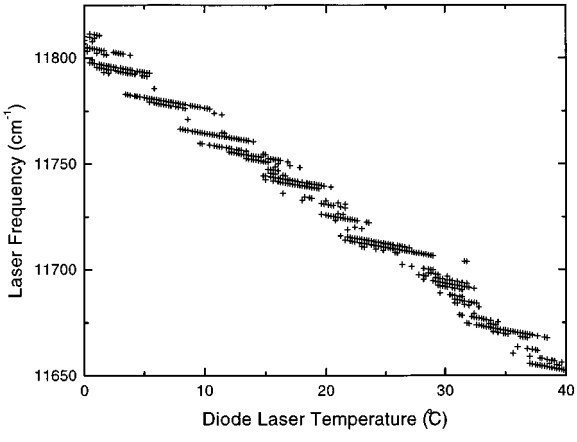

Fig. 4. Temperature-tuning characteristic of the 150-mW SDL-5400 diode laser was measured at a constant 130-mW power with the laser momentarily dropped below threshold to restart at each data point. Multiple modes are available at each temperature but nominally run one at a time. Which mode will appear after a current interrupt is random but is influenced by the phase of the field reflected from the collimating lens, which we mechanically control to force the laser to a particular mode. This characterization curve, with 0.2 °C steps, is automatically recorded and is used to find a preferred frequency pair for any required mid-IR frequency.

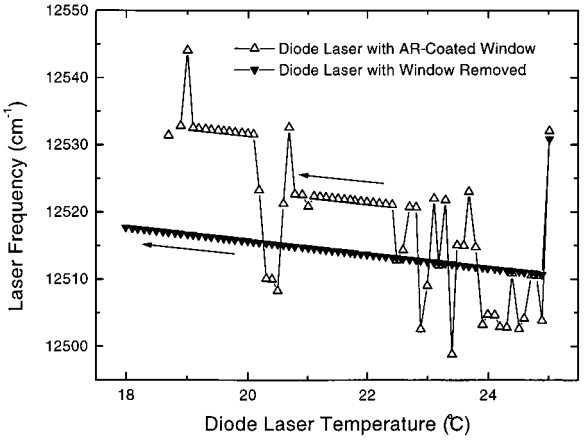

Fig. 5. The temperature tuning characteristic of one diode laser is vastly improved by removing the laser window. The SDL-5400 series 150 mW diode lasers have a pseudo AR coating on the emitting facet which increases the influence of reflected optical fields.

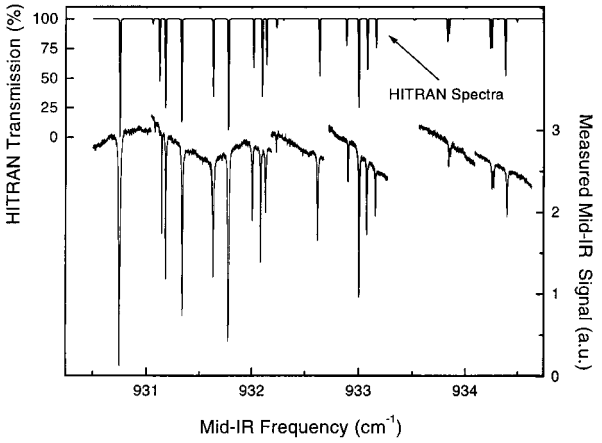

Fig. 6. NH_3 spectrum that was produced by combining a set of current-tuned scans, each of which was produced at a different (temperature-tuned) center frequency. The vertical displacements of the scans are intentionally not corrected. The HITRAN-based prediction of the spectra at the top of the figure corresponds well with our measured spectra.

puterized tuning sequence that steps the temperature by 0.2 °C from 0 to 40 °C and steps the current according to a predetermined matching ramp to maintain 130 mW. At each temperature step the current is repeatedly interrupted and the various resulting modal frequencies recorded. Each interruption also includes a change in the collimating-lens position. The data are automatically reduced to remove redundancies, and the result is shown in Fig. 4. The large temperature range used in the laser characterization process also requires automated adjustment of the laser lens to keep the beam collimated, and a CCD camera and New Focus picomirror to keep the beam aligned into a single-mode fiber for the wavemeter. Gaining access to several modes at each temperature, as shown in Fig. 4, provides denser and more consistent spectral coverage across the 40 °C tuning range.

The measured diode laser tuning curves are generally repeatable with multiple frequencies (modes) available at each temperature, but exhibit some randomness as well as some drift due to aging. The desired mode is obtained by repeated restarts of the laser with changes in the position of the collimating lens. The randomness is mostly avoided by the grading of every laser frequency in terms of its stability during the laser characterization stage and by the fact that there are hundreds of acceptable frequency pairs available. The slow frequency drift that is due to aging is accommodated by a change in the diode temperature if a histogram analysis of the recently available frequencies shows a collective shift ($<$1.5 °C).

B. Spectral Resolution and Scanning and Demonstration Spectra

Our system can produce continuous spectral scans between 11.8 and 16.1 μm by combining sections, as shown in Fig. 6 for NH_3. The resolution is better than 70 MHz. This is adequate for identifying and discriminating most Doppler-broadened molecular resonances. This continuous-scanning ability is accomplished despite the use of free-running near-visible lasers. The combined temperature tuning of the two diode lasers limited to the 0–40 °C region is 300 cm^{-1} that, with a better selection of their center frequencies, would allow tuning from 10.9 to 16.1 μm, limited by the 16-μm roll-off of our detector. Further, the addition of a third laser could triple the tuning range; for example, 790-, 850-, and 1015-nm diode lasers can pairwise provide DFG conveniently centered at 3.6, 5.2, and 11.1 μm.

The system has also passed the definitive test of spectrally scanning a list of 64 randomly chosen acetylene absorption lines between 12 and 15 μm without any human intervention. Figure 7 shows a single acetylene absorption line at 12.4 μm.

The current tuning rate of the 150-mW SDL diode lasers running at the 130-mW power level was ~1.6 GHz/mA. The smooth spectral scanning was ac-

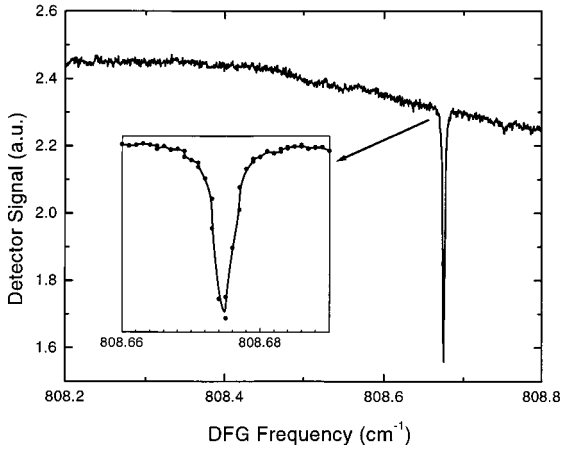

Fig. 7. Example of a low-pressure acetylene absorption line at 12.4 μm.

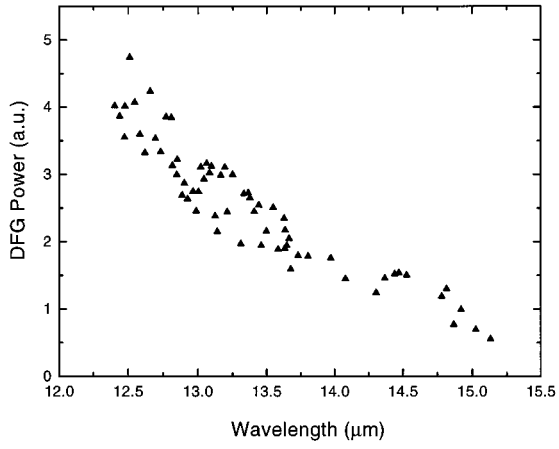

Fig. 8. Mid-IR power generated during the fully automated test of 64 randomly picked acetylene absorption lines shows a general decrease with increasing wavelength that is due to the inverse square wavelength dependence. The vertical scatter reveals the imperfect behavior of the automated power peaking system.

complished when the analog modulation inputs on the dual-laser current controller were driven from the analog output of the computer I/O board.

C. Tuning Range

Figure 1 shows that any frequency within the overall tuning range is accessible despite the mode-hopping behavior of the free-running drive lasers. This is demonstrated in Fig. 8, for which a list of 64 randomly chosen acetylene absorption lines between 12 and 15 μm was provided and the system automatically produced mid-IR sequentially at each frequency, spectrally scanned the absorption line, precisely located the line, and reported the fractional absorption without any human intervention. No lines were missed. The system checks for errors such as a mode hop during the scan and will then choose new frequency pairs until a successful spectral scan at every chosen frequency results.

The absolute frequency of the generated mid-IR power is known with an error of ~50 MHz. One consequence of this high precision is that a strong absorption line will prevent the mid-IR from being detected during the alignment and optimization steps; therefore a small frequency shift is added during the tuning phase and is then corrected when the absorption line is scanned.

The sequence of spectral scans is also recorded in convenient spreadsheet form, which is in turn presented by a program that permits the user to step rapidly through the spectra to identify particular features, for example, optical gain from a list of potential but yet untested plasma gain lines.

D. Power

The measured mid-IR output power is ~0.1 μW. The expected power is 0.5 μW. The input powers are roughly 100 mW each, which makes the conversion efficiency $\sim 10^{-6}$. Recently doped GaSe[15] has shown an improved conversion for thicker crystals but no change for thin crystals, which suggests that our conversion problem is a loss of phase matching over the 5-mm length due to lattice imperfections.

Figure 8 shows the mid-IR power versus the wavelength. The automated alignment for maximum power is revealed to be imperfect by the (vertical) variation in power at a given wavelength. The power is expected to decrease with increasing wavelength because of an intrinsic inverse square dependence on the mid-IR wavelength. The power in Fig. 8 is corrected for the detector response, but the detector rolls off sharply at 16 μm, which limits our current spectrometer to an upper wavelength of 16.1 μm.

E. Automation

The system is fully automated, including the selection of the optimal drive laser frequencies, tuning the diode lasers to the correct frequencies, aligning the beams in the nonlinear crystal, setting the crystal angle, detecting the IR signal, optimizing the mid-IR power, spectrally scanning the region, and locating and evaluating the absorption line found in the scan. Errors in optical alignment are corrected from the beginning of the system to the end of the system, from the near-visible diode laser drivers to the mid-IR detector. The automation of the whole system was thoroughly exercised during the test scan of the 64 acetylene absorption lines between 12 and 15 μm, which was accomplished without error.

This successful automation gives the system its primary virtue, the ability to perform an unlimited series of laser-based spectroscopic tasks more rapidly and probably with a much greater chance of success then can be accomplished by human control of the system. This virtue permits testing, for example, all the possible energy-level pairs in a He–Ne plasma for overlooked IR gain lines, a task undoubtedly previously rejected in part because of the amount of human labor involved. The successful automation now makes possible many such previously unapproachable problems. The system is also a large step toward a universal laser-based air-pollution monitor, which sequences through a large set of known or simply suspected trace gases. The present status of high-sensitivity laser-based detection of multiple trace gases is limited to, at best, two or three different molecules that are conveniently close in frequency and can be captured by a single current scan of a lead-salt laser or by multiple scans of multiple lasers.[19]

5. Algorithms

In this section the LabView software language, automated optical adjustments, tuning the free-running diode lasers, and processing of the spectral-scan data are discussed.

A. LabView Software

The spectrometer was built with LabView, which is an object-oriented programming language in which icons that represent subprograms have (electriclike)

terminals that are wired together to indicate variables and data flow. This differs from a command-line language in that program steps can occur in any sequence, waiting only for the necessary new data to appear. This data-dependent language was extremely effective and certainly seemed to simplify and make possible, in the limited time span, the design and the testing of the complicated spectrometer for which 300 programs were written. The language also greatly facilitated data manipulation and graphing, communication with laboratory instruments, and the I/O of analog signals.

B. Automated Optical Alignment and Optimization

1. Drive-Beam Alignment into the Nonlinear Crystal

Four motorized mirrors are used to set the position and the angle of the two input beams. Figure 2 shows the focusing lens separated by one focal distance from the nearest picomirror: this spacing permits this mirror to move the position of one beam at the crystal without changing its angle of approach. The optimum-approach angles of the two drive beams are different primarily because of the different optical indices for the ordinary and the extraordinary beams combined with the large approach angle (roughly 45°). Also, the two beams are displaced at the crystal entrance to partially correct for the walk-off (typically 48 mrad) of the extraordinary beam inside the crystal. The second adjustment mirror for each drive beam is several focal distances away from the focusing lens to minimize its effect on the beam position at the crystal while adjusting the angle of approach. The same angle of approach and beam positions are used throughout the tuning range of 11.8–16.1 μm.

The compact CCD cameras (without lenses) are used to gauge the position and the angle of approach of the two drive beams. A motorized deflector mirror is inserted into the focused beam path, and one camera is positioned at the equivalent (focused) position of the crystal to gauge the beam position. The second camera is imaged with a simple lens to a position 60 mm before the crystal to gauge the angle of approach. The deflector mirror is constructed from a magnetic-head drive mechanism as extracted from a failed computer hard drive and has excellent repeatability. The CCD cameras feed a framegrabber board inside the control computer, and the images are processed to determine the diode laser beam locations. The processing consists primarily of thresholding and low-pass filtering to remove background noise and the extended wings of the imperfect diode laser beam shapes that can significantly affect the two-dimensional center-of-mass calculation.

The beam-positioning corrections are passed to the picomirror controller (New Focus) through an IEEE GPIB, and the cycle is repeated, typically six times, until one-half pixel errors result (~4 μm at the cameras). The complete two-beam-alignment process, which uses a 166-MHz Pentium CPU and a slow framegrabber that transfers 1 byte per cycle, takes ~2 min. No special signal processing for this feedback loop is necessary since no time constants are involved, other than paying attention to the size of correction (gain) during each cycle and the coupled effects of the tandem adjustment mirrors on each beam. Since neither hysteresis nor nonmonotonic behavior is a problem in this particular beam-alignment feedback system, we can correct noise or actuator resolution problems by loosening the one-half pixel requirement, by reducing the fraction of the error that is corrected during each cycle, and by using more data averaging.

2. Diode Laser Collimation-Lens Adjustment

The 0–40 °C span used to temperature tune the 809- and the 856-nm diode lasers excessively changes the relative position of the collimating lenses in the Newport diode laser mounts. This was measured as −0.47 μm/°C and was compensated for by a motorized swing arm mounted on the rotating lens mount, which was set based on the known diode laser temperature. The frame temperature, despite being bolted to an optical table, also affects the collimating-lens spacing and was measured to have a rate of 0.74 μm/°C.

The collimating-lens mount uses 80-turns/in. threads and exhibits a rocking motion that is significantly reduced when the threads are filled with a stiff, nonmelting high-vacuum grease. The remaining rocking motion, plus any flaw in the lens concentricity with the laser, deflects the exiting beam, which is corrected with one common CCD camera and one picomirror each for the two diode lasers. This keeps the drive beams aligned as they subsequently traverse the optical table, as well as aligning them into a common single-mode optical fiber that feeds the wavemeter for absolute frequency information and the scanning Fabry–Perot spectrum analyzer for sidelobe-noise information.

The collimating lens is also adjusted in increments of ~0.125 μm to reduce the diode laser's sidelobe noise (typically at the relaxation oscillation frequency, 1–3 GHz) by a change in the phase of the optical reflection returning to the laser from the lens. This effect is significantly more pronounced when low-facet-reflectivity 150-mW SDL diode lasers are used instead of natural-reflectivity 50-mW Sharp lasers. The sidelobe-noise level is extracted from the analog data stream that comes from the scanning Fabry–Perot by identification of the primary spectral component and a comparison of it with other peaks spaced appropriately from the strongest peak.

Finally, one infrequently used program correctly adjusts the collimating-lens position without regard to the expected temperature relationship by repeatedly fitting a Gaussian profile to the beam shape and resetting the collimating lens until the proper beam radius is obtained. This program then updates the temperature-dependence formula that is used routinely to predict the proper lens position.

3. Automatic Optimization

The laser spectrometer uses optical optimization routines on only the crystal angle and the alignment of the mid-IR detector to maximize the infrared power.

A critical issue in optimizing a mirror or the crystal angle is the signal-to-noise ratio (SNR). For example, the automated observation that there is in fact any mid-IR signal is accomplished by the requirement of a minimum SNR, measured by a program that samples the signal stream, operates a motor beam block, samples the zero reference signal, and calculates the standard deviation. This in fact mimics the human technique. If the SNR is too low, the integration time is increased to a maximum of 60 s. Once the signal is found, a minimum integration time is calculated and used while the optimization is performed. For example, if the signal level changes by less than the integrated-noise level, it is then treated as a zero change so as not to provide confusing feedback.

4. Optimizing the Crystal Angle

The angle-tuning sensitivity shows a FWHM of $\sim 0.4°$. The phase-matched crystal angle is calculated based on improved Sellmeier coefficients[17] and set with a resolution better than 0.01° by the compact motorized rotary mount (National Aperture) and a sequence that reduces mechanical hysteresis by first causing the rotary mount to overshoot the desired angle by a fixed amount and then second by approaching the desired angular position slowly and always from the same direction.

We optimize the crystal angle by stepping the angle in one direction until a believable decrease in signal level takes place and then changing direction. A minimum step size of 0.05° is used to reduce the probability of a false reversal that is due to a small local maximum. The measured signal levels and corresponding crystal angles are then fitted to a parabola, and the peak of this parabola is used as the optimum angle. This permits us to use a relatively large step size while also accurately locating the peak. Finally the formula used to predict the crystal angle is updated if its error is greater than 0.08°.

5. Optimizing the Mid-IR Beam into the Detector

Maximizing the detected signal by use of the two picomirrors in tandem that feed the detector is complicated by the fact that the signal shows multiple peaks because of an imperfect beam shape and etalon effects in the detector window. Our solution is to step the mirror in one direction, with a step size large enough to not be trapped by most local maxima, until the peak is passed, and to backstep once. This simple algorithm was found to be superior to fitting the detected signal and mirror position to a parabola as is done with the crystal angle, in part because, without a position encoder, the picomirror position is not accurately known because of its randomly different clockwise and counterclockwise speeds and because of the strong local maxima that disturb the parabolic fit made with a limited number of data points. The overall result is an imperfect optimization, as shown in Fig. 8 by the vertical scatter in the mid-IR power data points at any particular wavelength.

C. Tuning

Tuning the two free-running 800–900-nm diode lasers with an accuracy of 0.01 cm^{-1} is a complicated process and is described below. In short, two frequency look-up tables that give the optical frequencies of the diode lasers as functions of temperature are compared and an exhaustive list is compiled of pairs of frequencies that give the desired mid-IR frequency; the best frequency pair is then chosen in terms of stability, which includes the current- and the temperature-tuning ranges without a mode hop and frequency repeatability, as well as sidelobe noise, probability of acquiring those frequencies, the smallest error in generating the desired mid-IR frequency, and the smallest required temperature tuning; then the lasers are set to the chosen temperatures and currents; the lasers' frequencies are measured by the wavemeter (0.001 cm^{-1}), the laser current is momentarily kicked down below threshold to restart the laser, the collimating lens is moved in steps of 0.125 μm to change the optical feedback, and the desired output frequency is tested for current tuning to resist mode hops, for frequency stability, and for sidelobe-noise energy; and finally current tuning is used to move the two diode laser frequencies until the expected difference frequency is within 0.01 cm^{-1} of the desired mid-IR frequency.

1. Frequency Look-Up Tables

The look-up tables are previously generated by a scan of the diode laser temperature by 0.2 °C steps from 0 to 40 °C while the current is changed to keep the power approximately constant at 130 mW. The laser collimating lens is stepped six times, and with the diode current kicked below threshold before each measurement, the optical frequency, sidelobe-noise fraction, temperature-tuning range (± 0.2, ± 0.5 °C), and current-tuning range (± 2, ± 5 ma) are recorded. These data at each temperature location are reduced to remove redundancies and to give a stability measure, best sidelobe-noise behavior, and the number of times a particular frequency appears. This automated laser characterization program also records the data in the convenient spreadsheet form.

2. Find Frequency Pairs

The two frequency look-up tables for the two lasers are processed to find all combinations of frequencies whose difference is within 0.1 cm^{-1} of the desired mid-IR frequency. There are typically greater than 100 such pairs, as shown in Fig. 1. A new list in spreadsheet form containing these pairs is assembled and handed to the program, which picks the best pair.

3. Choose Best Frequency Pair

This program attempts to find a pair that matches all the preferred criteria, but backs down the require-

ments as needed in a predefined sequence. There are five levels of stability, two levels of mid-IR frequency accuracy, two levels of sidelobe noise, two levels of frequency repeatability (pick a mode that is dominant), two levels of required temperature change (stay near 25 °C if possible), and two levels of frequency deviation from the linear approximation to the frequency–temperature map (stay near the most likely center frequency for a given temperature).

4. Force Lasers to Chosen Frequencies

The free-running diode lasers with Fabry–Perot cavities can typically operate at several different longitudinal modes for each temperature and fixed current. Our technique is to kick down the diode laser current below threshold momentarily to permit the laser to restart. The collimating-lens position is also sequenced to improve the stability (and probability of acquisition) at the desired frequency. If the desired frequency is acquired, the laser is checked for frequency wander, sidelobe-noise level, and stable current tuning. If the frequency is not acquired during the 48 attempts, a histogram analysis is performed on the frequency errors to determine if a small temperature tuning ($<$1.5 °C) could reach the desired frequency, assuming that the correct mode can be reacquired; this accommodates a slow shift in the frequency-tuning curve that appears to be due to aging. Failure here to obtain the correct diode laser frequencies involves rerunning the program to choose the best frequency pair, with the failed frequency pair(s) removed. Success here concludes with a fine current tuning of both lasers to achieve an initial mid-IR frequency error below 0.01 cm^{-1}.

D. Spectral-Scan Processing

Present high-resolution trace-gas monitoring systems that use lead-salt lasers require sophisticated personnel to exactly set the laser frequency, which is typically accomplished by observation of a known pattern of nearby absorption lines, and to position the primary absorption line such that the data-processing algorithm can remain locked. Our tunable mid-IR spectrometer performs these functions automatically.

Our mid-IR source is first set to be accurate to 0.01 cm^{-1} or 300 MHz, although it can be set to a higher resolution if needed. The frequency scan used in the acetylene demonstration of 64 absorption lines was ~4.25 GHz each, which guarantees that the intended absorption line is within the scan and centered with an accuracy of ~7%. The precise position of the absorption line in the scan data is determined by a Fourier-transform matched filter, which is quite effective under noisy conditions, especially if the width of the absorption line used in the design of the matched filter is set to be equal to or, if not precisely known, to be larger than the expected width. This identification and position-determining step also yields estimates of the background-signal level, background tilt, and depth of the absorption line, which are used as initial guesses in the subsequent nonlinear fitting routine. Fixing the location of the absorption dip by the matched filter greatly improves the stability of the nonlinear fitting routine, which adjusts the following parameters: absorption linewidth, absorption depth, background-signal level, and background tilt. The effect is a robust algorithm for extracting the fractional absorption from noisy scans. We can further improve the routine in terms of noise resistance by more accurately (50 MHz) setting the initial mid-IR frequency and then by allowing only a small correction to the precise position of the absorption line to be made by the matched filter. This would be especially attractive for automating the measurement of weak absorption lines in a noisy background in which random-noise dips might otherwise be incorrectly identified as the absorption line.

The spectral scans and the extracted fractional absorption were recorded in a spreadsheet format, and a LabView program was prepared to permit the user to step through a graphical presentation of the finished spectral scans rapidly and conveniently.

6. Conclusion

IR absorption is a widely applicable method of sensitively detecting small quantities of gases in the atmosphere since nearly all molecules absorb in the mid-IR 3–20-μm region. The conventional approach for measuring these trace gases is with a tunable IR diode laser. These lasers are somewhat unreliable and typically require liquid-N_2 cooling. Also, these systems generally have a very narrow tuning range that limits them to measuring, at best, a few different molecules. The final and most critical problem is the lack of automated alignment including detectors and the multipass cell, and precise and repeatable frequency tuning of the laser, which unfortunately then requires the attention of technically adept personnel who are trained on the specific system.

Our mid-IR spectrometer reported here also measures IR absorption features but uses dependable, near-visible room-temperature diode lasers to make a cw narrow-bandwidth source that is continuously tunable from 11.8 to 16.1 μm and has fully automated optical alignment, frequency tuning, and data processing. Our IR source is based on nonlinear difference-frequency mixing of the two diode lasers and is rapidly and smoothly tunable over ~2 cm^{-1} and, when spectral sections are patched together, can be continuously tuned over 300 cm^{-1}. Computer-operated frequency control uses temperature and current tuning of the free-running diode lasers by means of previously recorded reference tables with a complex tuning algorithm, including absolute frequency data from a wavemeter and spectral-noise information from a scanning Fabry–Perot spectrum analyzer. The system has been demonstrated by successfully scanning, without any human intervention, 64 randomly selected acetylene absorption lines between 11.8 and 16 μm. A scan of a single acetylene absorption line and a composite spectral scan of NH_3 with a 70-MHz resolution were also presented.

Tunable mid-IR diode laser absorption spectroscopy has developed over the past 20 years into a sensitive trace-species-detection method for environmental, combustion, and industrial process problems, as well as fundamental spectroscopy studies. However, it has been largely confined to research applications because of the high degree of expertise required for operating cryogenic lead-salt diode lasers. Our mid-IR spectrometer demonstration shows that it is possible to extend the range of applications beyond specialized research areas and make this technique feasible for routine monitoring of multiple trace-gas species simultaneously by technically unsophisticated personnel: Potential applications include environmental air quality and atmosphere composition measurements, toxic-gas detection, pollution emission source monitoring, soil gas composition determination, and process control in plasma and chemical vapor deposition reactors. The successful automation gives our system its primary virtue: the ability to perform an unlimited series of laser-based spectroscopic tasks more rapidly then can be accomplished by human control.

The authors and their research were supported by the U.S. Department of Energy, contract DE-FG02-94ER-81698, through Aerodyne Research, Inc.

References

1. C. E. Kolb, J. C. Wormhoudt, and M. S. Zahniser, "Recent advances in spectroscopic instrumentation for measuring stable gases in the natural," in *Biogenic Trace Gases: Measurement Emissions from Soil and Water*, P. A. Watson and R. C. Harriss, eds. (Blackwell Science, Oxford, U.K., 1995), pp. 259–290.
2. D. J. Brassington, "Tunable diode laser absorption spectroscopy for the measurement of atmospheric species," in *Spectroscopy in Environmental Science*, R. E. Hester and R. S. Clark, eds., Vol. 24 of Advances in Spectroscopy Series (Wiley, New York, 1995).
3. J. Faist, F. Capasso, D. L. Sivco, C. Sirtori, A. L. Hutchinson, and A. Y. Cho, "Quantum cascade laser," Science **264,** 553–556 (1994).
4. R. Q. Yang, B. H. Yang, D. Zhang, C.-H. Lin, S. J. Murry, H. Wu, and S. S. Pei, "High power mid-infrared interband cascade lasers based on type II quantum wells," Appl. Phys. Lett. **71,** 2409–2411 (1997).
5. K. Namjou, S. Cai, E. A. Whittaker, J. Faist, C. Gmachl, F. Capasso, D. L. Sivco, and A. Y. Cho, "Sensitive absorption spectroscopy with a room-temperature distributed-feedback quantum-cascade laser," Opt. Lett. **23,** 219–221 (1998).
6. W. R. Bosenberg, A. Drobshoff, J. I. Alexander, L. E. Myers, and R. L. Byer, "93% pump depletion, 3.5-W continuous-wave, singly resonant optical parametric oscillator," Opt. Lett. **21,** 1336–1338 (1996).
7. A. S. Pine, "Doppler-limited molecular spectroscopy by difference-frequency mixing," J. Opt. Soc. Am. **64,** 1683–1690 (1974).
8. U. Simon, F. K. Tittel, and L. Goldberg, "Difference-frequency mixing in $AgGaS_2$ by use of a high-power GaAlAs tapered semiconductor amplifier at 860 nm," Opt. Lett. **18,** 1931–1933 (1993).
9. R. S. Putnam, "Diode laser difference frequency detects ammonia and chlorofluorocarbons at 11.5 microns," in *Conference on Lasers and Electro-Optics*, Vol. 9 of 1996 OSA Technical Digest Series (Optical Society of America, Washington, D.C., 1996), pp. 13–14.
10. R. S. Putnam, "Applying room temperature diode lasers to difference frequency generation," in *Intracavity and Extracavity Control of Laser Beam Properties*, R. L. Facklam, K. H. Guenther, and S. P. Velsko, Proc. SPIE **1869,** 242–249 (1993).
11. U. Simon, C. E. Miller, C. C. Bradley, R. G. Hulet, R. F. Curl, and F. K. Tittel, "Difference-frequency generation in $AgGaS_2$ by use of single mode diode laser pump sources," Opt. Lett. **18,** 1062–1064 (1993).
12. K. P. Petrov, L. Goldberg, W. K. Burns, R. F. Curl, and F. K. Tittel, "Detection of CO in air by diode-pumped 4.6-μm difference-frequency generation in quasi-phase-matched $LiNbO_3$," Opt. Lett. **21,** 86–88 (1996).
13. N. C. Fernelius, "Properties of gallium selenide single crystal," Prog. Cryst. Growth Charact. **28,** 275–353 (1994).
14. A. E. Siegman, *Handbook of Nonlinear Optical Crystals*, ed., (Springer-Verlag, New York, 1991), pp. 87–88.
15. D. R. Suhre, N. B. Singh, V. Balakrishna, N. C. Fernelius, and F. K. Hopkins, "Improved crystal quality and harmonic generation in GaSe doped with indium," Opt. Lett. **22,** 775–777 (1997).
16. U. Simon, Z. Benko, M. W. Sigrist, R. F. Curl, and F. K. Tittel, "Design considerations of an infrared spectrometer based on difference-frequency generation in $AgGaSe_2$," Appl. Opt. **32,** 6650–6655 (1993).
17. W. C. Eckhoff, R. S. Putnam, S. Wang, R. F. Curl, and F. K. Tittel, "A continuously tunable long-wavelength cw IR source for high-resolution spectroscopy and trace gas detection," Appl. Phys. B **63,** 437–441 (1996).
18. Source of GaSe crystal: Eksma Co., Vilnius, Lithuania, eksma@auste.elnet.lt.
19. J. Wormhoudt, M. S. Zahniser, D. D. Nelson, J. B. McManus, R. C. Miake-Lye, and C. E. Kolb, "Infrared tunable diode laser measurements of nitrogen oxide species in an aircraft engine exhaust," in *Optical Techniques in Fluid, Thermal, and Combustion Flow*, S. S. Cha and J. D. Trolinger, eds., Proc. SPIE **2546,** 552–561 (1995).